Acta Automatica Sinica
Vol. 33, No. 3 March, 2007
DOI: 10.1360/aas-007-0286

Computer Vision-based Navigation and Predefined Track Following Control of a Small Robotic Airship

XIE Shao-Rong[1] LUO Jun[1] RAO Jin-Jun[1] GONG Zhen-Bang[1]

Abstract For small robotic airships, it is required that the airship should be capable of following a predefined track. In this paper, computer vision-based navigation and optimal fuzzy control strategies for the robotic airship are proposed. Firstly, visual navigation based on natural landmarks of the environment is introduced. For example, when the airship is flying over a city, buildings can be used as visual beacons whose geometrical properties are known from the digital map or a geographical information system (GIS). Then a geometrical methodology is adopted to extract information about the orientation and position of the airship. In order to keep the airship on a predefined track, a fuzzy flight control system is designed, which uses those data as its input. And genetic algorithms (GAs), a general-purpose global optimization method, are utilized to optimize the membership functions of the fuzzy controller. Finally, the navigation and control strategies are validated.

Key words Visual navigation, flight control, predefined track following, robotic airship.

1 Introduction

Small airships are aerial robots built from a lightweight envelope for buoyancy and a propelling system housed in a gondola. The fact that the flight of airships is based on buoyancy is one of their main advantages. Small airships outperform sub-miniature fixed-wing vehicles (airplanes) and rotary-wing aircrafts (helicopters) in stability, operation safety, endurance, payload to weight ratio[1], *etc.* So they will surely find uses in[2∼3] anti-terrorism, traffic observation, advertising, aerophotogrammetry, climate monitoring, locale of calamity watching, surveillance over man-made structures and archaeological sites, as well as establishment of emergency telecommunication relay platforms. For these missions, it is demanded that the airship is capable of autonomously following predefined track, which consists of autonomous navigation and flight control. Consequently, they are recently becoming a focus of research.

The accomplishments of the above tasks make visual sensors (like CCD cameras) a natural choice for their sensory apparatuses. Visual sensors are necessary not only to the performances data acquisition as part of the mission such as taking pictures of predefined spots, but also to autonomous navigation of the small airship, supplying data in situations where conventional, well-established aerial navigation techniques, like those using inertial, GPS and other kinds of dead-reckoning systems, are not adequate.

There have been important developments in the area of visual navigation for mobile robots in recent years. Among those more successful are the ones that use navigation based on visual landmarks[4]. For aerial robots, though previous work on visual servoing has comprised the stabilization problem[5∼6] and vertical landing[7] using small indoor blimps and helicopters, hovering solution[8] and a strategy for line-following tasks[9∼11] using outdoor robotic airships, visual navigation of aerial robots is much less explored[12]. Usually, autonomous navigation of UAVs relies on inertial navigation system (INS), GPS, DGPS, *etc.*, which are traditional and well-established in navigation of aircraft in general. It is clearly understood that vision is in itself a very hard problem and solutions to some specific issues are restricted to constraints either in the environment or in the visual system itself. Nevertheless, visual navigation could be of great advantages when it comes to aerial vehicles in the aforementioned situations.

Fig. 1 The airship in Shanghai University

In the present paper, visual navigation of a small robotic airship based on natural landmarks already existent in the environment is introduced. The vision system is able to track those visual beacons. For example, buildings can be used as visual beacons when the airship is flying over a city. According to the digital map or the geographical information system (GIS), their geometrical properties are known. Then a geometrical methodology can extract information about orientation and position of the airship. And in order to keep the airship on a predefined track, an optimal fuzzy flight control system is designed, which uses that data as its input.

2 Dynamic characteristics and control architecture of the small robotic airship

The prototype of the robotic unmanned blimp we developed is shown as Fig. 1. The platform has a length of 11 m, a maximal diameter of 3 m, and a volume of 50 m^3. It is equipped with two engines on both sides of the gondola, and has four control surfaces at the stern, arranged in a '+' shape. Its useful payload capacity is around 15 kg at sea level. It can flight with a maximum speed of about 60 km/h.

The mathematical, reasonable and relatively simple linear dynamic model of the small robotic airship is readily

Received August 12, 2005; in revised form February 16, 2006
Supported by National Natural Science Foundation of P. R. China (50405046, 60605028), Shanghai Project of International Cooperation (045107031) and the Program for Excellent Young Teachers of Shanghai (04Y0HB094).
1. School of Mechatronics Engineering and Automation, Shanghai University, Shanghai 200072, P. R. China

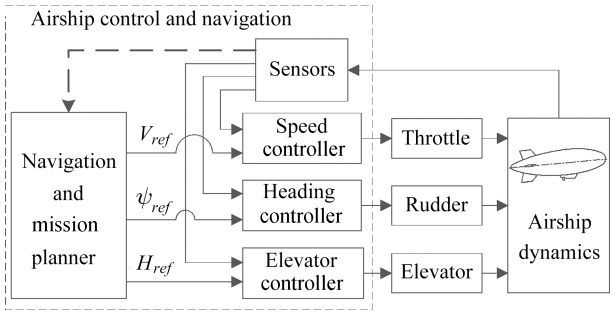

Fig. 2 Architecture of control and navigation system

analyzed and realized. The airship dynamics indicates that the state parameters involved in longitudinal and lateral motions are weakly dependent. So the system can be split into two subsystems in the following way.

1) $S_{long} = [X, Z, \theta]^{\mathrm{T}}$ and $S_{long} = [U, W, Q]^{\mathrm{T}}$ to describe the dynamics within the longitudinal plane, the control inputs being δ_e and δ_t.

2) $S_{lat} = [Y, \phi, \psi]$ and $X_{lat} = [V, P, R]^{\mathrm{T}}$ to describe the dynamics within the lateral plane, the control input being δ_r.

The body axes are fixed in the vehicle with the origin O at the center of volume (CV), the OX axis is coincident with the axis of symmetry of the envelope, and the OXZ plane coincides with the longitudinal plane of symmetry of the blimp. (ϕ, θ, ψ) denote three Euler angles. The airship linear and angular velocities are given by (U, V, W) and (P, Q, R), respectively.

The airship dynamics model shows that: 1) The rolling corresponding mode is structurally stable. 2) The longitudinal and lateral control can be viewed as decoupled. 3) An airship has more nonlinearities than ordinary aircraft due to the added mass.

According to that decoupled lateral and longitudinal dynamics model, the control architecture of the system is presented in Fig. 2.

In this architecture three independent controllers are utilized as follows. 1) A proportional-integral controller for the longitudinal velocity v acting on the throttle deflection δ_t; 2) a heading controller acting on the rudder deflection δ_r; 3) a controller for height and pitch acting on the elevator deflection δ_e.

The navigation and mission planner is designed to provide longitudinal velocity reference V_{ref} height reference H_{ref} and heading reference Ψ_{ref}. In a specific mission flight, , H_{ref} and the waypoints are predefined by the user. As the airship position is motional, the planner should be computed in real-time for the heading controller.

3 Visual navigation methodology

3.1 Navigation principle based on visual beacon[12]

Visual beacons denote calibration objects with known visual and geometrical properties. Formally, the beacon visually assigns a set $\{P_0, P_1, P_2, P_3\}$ of characteristic points where the distances of the form $\|\vec{P}_i - \vec{P}_j\|$, $0 \le i < j < n$ are known.

Depending on the number and disposition of the characteristic points, it is possible to use an image of the beacon - acquired by an onboard camera with known parameters (focus, resolution, CCD physical dimensions) - to estimate the position and orientation of that camera, and consequently of the airship, in relation to the visual beacon.

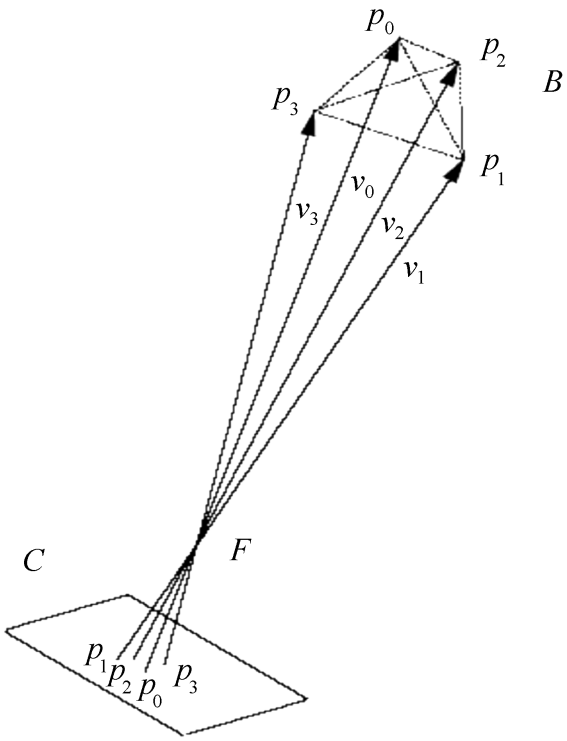

Fig. 3 Image projection of the vertices of a tetrahedral beacon B over the image plane of camera C

Fig.3 illustrates the geometrical construct of image projection. Let C be a camera with focal point F. Let B be a visual beacon with a set of 4 non-coplanar characteristic points $\{P_0, P_1, P_2, P_3\}$. Let $\{p_0, p_1, p_2, p_3\}$ be the coplanar points corresponding to the image projections of the characteristic points of B over the image plane of C. Let $\vec{V}_i = P_i - p_i$, $0 \le i < 4$, be the light-ray-path vectors going from the points p_i to the corresponding P_i passing through F, and $\vec{v}_i = F - p_i$, $0 \le i < 4$, the vectors in the same direction of V_i, but going just until F.

Once the vectors $\vec{V}_i$ are found, the position and orientation of C can be determined. Since the distances between the points P_i are known and vectors $\vec{v}_i$ are determinable if the points p_i are known, the following equation system (1) can be specified, where $D_{i,j} = \|P_i - P_j\|$, $0 \le i < j \le 3$, is the distance between points P_i and P_j. The unknowns of the system are $\lambda_0, \lambda_1, \lambda_2, \lambda_3$ and $\vec{V}_i = \lambda_i \vec{v}_i$. Expanding the modulus operations on the left-hand side of the equation, we have a nonlinear system with six quadratic equations and four unknowns as follows:

$$\begin{cases} \|\lambda_0\vec{v}_0 - \lambda_1\vec{v}_1\| = D_{0,1} \\ \|\lambda_0\vec{v}_0 - \lambda_2\vec{v}_2\| = D_{0,2} \\ \|\lambda_0\vec{v}_0 - \lambda_3\vec{v}_3\| = D_{0,3} \\ \|\lambda_1\vec{v}_1 - \lambda_2\vec{v}_2\| = D_{1,2} \\ \|\lambda_1\vec{v}_1 - \lambda_3\vec{v}_3\| = D_{1,3} \\ \|\lambda_2\vec{v}_2 - \lambda_3\vec{v}_3\| = D_{2,3} \end{cases} \quad (1)$$

The existence of the six equations guarantees one solution. Therefore, a visual beacon with tetrahedral topology - that

is, having four non-coplanar characteristic points - guarantees a unique solution to the values $\vec{V}_i$, hence a unique position and orientation to the camera for the point set p_i determined in an image.

However, tetrahedral - and therefore tridimensional - beacons are more difficult to construct and reproduce than the bidimensional ones; in particular, practical applications of autonomous airships, where the distances involved could be large and hence the visual beacon, seem to favor the use of bi-dimensional ones. A bi-dimensional beacon would have to have a minimum of three characteristic points to make possible the determination of position and orientation of the camera since with points less than thrice the number of solutions found for position and orientation would be infinite. Nonetheless, a triangular beacon would imply in an equation system just three quadratic equations, in a way the number of solutions for a given projection of characteristic points on the image plane would be 2 or 4. That is, for a given image of a triangular beacon, there would be two or four possible positions /orientations of the beacon with the same characteristic point projections found in the image. However, this ambiguity can be removed if distortions in the vertex markers, caused by perspective projection, are taken into account. Observing the apparent size of each marker, it is possible to determine the ratios between their distances and thus to choose one among the several solutions.

3.2 Implementation of Visual Navigation

According to the above principle, it is very important that the point set p_i be determined by digital image processing method for implementation visual navigation. Because p_i is the point corresponding to the image projection of the characteristic point of natural visual beacon over the image plane of C, feature-based approaches are ideal for picking up feature points of natural beacons. They are successfully carried out in computer vision. For example, when the airship is flying over a city, buildings can be used as visual beacons, as their feature points easily are segmented in images. According to the digital map of the city or the geographical information system (GIS), their geometrical properties are known. In general, they are shown in a graphical interface (Fig.4 block 3, see next page).

The camera coordinate system $\{C\}$ is presented in first place. That system is an orthonormal basis with the CCD matrix center as the origin, X axis parallel to the CCD width, Y axis parallel to the CCD height and Z axis coincident with the camera axis (line perpendicular to the image plane passing through the focal point), pointing toward the back of the camera. On the other hand, $\{B\}$ is the world coordinate system.

The geometrical methodology used here for computing estimations of position and orientation of the airship from an onboard camera is simple. Since the onboard camera is assumed to be installed at the bottom of the airship gondola, pointing downwards, and the $X-Y$ plane of $\{B\}$ is parallel to the image plane, the yaw orientation is easily determined.

4 Optimal fuzzy control system

4.1 Heading controller

The control block of the heading controller is shown in Fig.5. The heading controller consists of a rule based fuzzy controller and an integrator.

The integrator (Fig.5 block (b)) is used to include the integral of the error as a third input to the heading controllers to compensate for setpoint error caused by unbalanced forces and other disturbances. The integrator is reset at zero on each change of setpoint. Because integration only occurs for small values of error, the problems of integrator windup are avoided and at the same time the setpoint is eliminated.

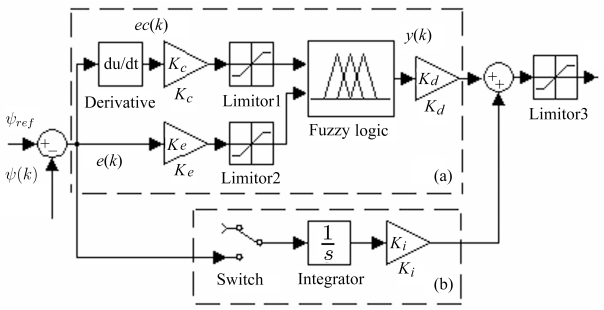

Fig. 5 Heading controller block diagram

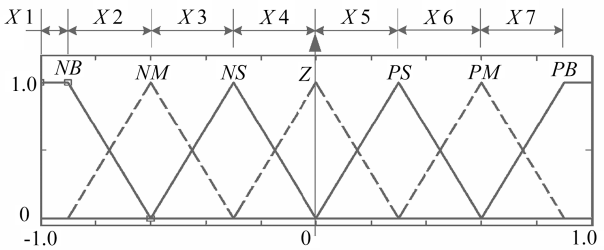

Fig. 6 The membership functions for the fuzzy input

The fuzzy controller (Fig.5 block (a)) is the main part of the heading controller. Its inputs are heading error and heading error rate , and the output is δ_r. K_e and K_c are normalized from the universes of discourse of the inputs to the range of [-1, 1]. The universe of discourse of output deflection is limited in [-30deg, 30deg] by the actual mechanism of the control surfaces, so $K_d = 30$. Seven fuzzy sets are defined for each input variable, as shown in Fig.6, where $x_1 = 0.1$ and $x_i = 0.3$ $(i = 2, 3, \cdots, 7)$ for the initial design. The rule base is built as shown in Table 1.

4.2 Optimization of Fuzzy Controller

Since the rule base and membership functions of fuzzy set are determined by designers imprecisely, the quality of control may be not that good. So a tuning operation is needed for the fuzzy control system. In fact, this operation is a process of optimization. Genetic algorithms (GAs), known to be robust general-purpose global optimization method, are utilized to optimize the membership functions of fuzzy controller.

Considering Fig.6, the membership functions of two fuzzy input variables are determined by parameters $x = (x1, x2, \ldots, x14)$ of a controller, where $x1, x2, \ldots, x7$ for error and $x7, x8, \ldots, x14$ for error rate. In this approach constraint conditions are inducted to guarantee that all fuzzy sets are in the universes of discourse.

$$g_1 = \sum_{i=1}^{7} x_i - 2 \leq 0 \tag{2}$$

$$g_2 = \sum_{i=8}^{14} x_i - 2 \leq 0 \tag{3}$$

where g_1 and g_2 are functions of constraint.

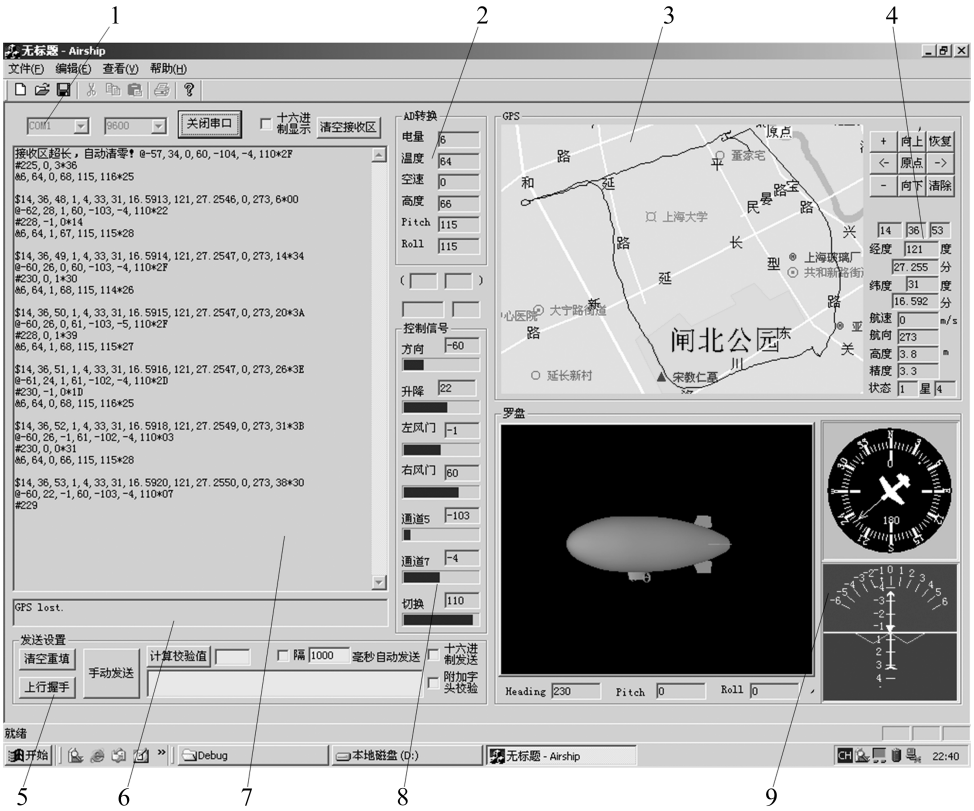

1) COM setting; 2) A/D data; 3) Digital map and flight trajectory; 4) GPS data; 5) Command editor; 6) Error prompt; 7) Flight data; 8) Control inputs; 9) Flight attitude

Fig. 4 The human-machine interface of ground station

Table 1 Fuzzy rule base

$EC\backslash E$	NB	NM	NS	Z	PS	PM	PB
NB	-0.8333	-0.8333	-0.6333	-0.5	-0.3333	-0.1667	0
NM	-0.8333	-0.6333	-0.5	-0.3333	-0.1667	0	0.1667
NS	-0.6333	-0.5	-0.3333	-0.1667	0	0.1667	0.3333
Z	-0.5	-0.3333	-0.1667	0	0.1667	-0.3333	0.5
PS	-0.3333	-0.1667	0	0.1667	0.3333	0.5	0.6333
PM	-0.1667	0	0.1667	0.3333	0.5	0.6333	0.8333
PB	0	0.1667	0.3333	0.5	0.6333	0.8333	0.8333

In traditional GAs, the optimization problems with constraint conditions are converted into the ones without constraint conditions using penalty functions. But it's not easy to determine the penalty coefficients. When the penalty coefficients are small, some individuals out of the searching space may have high fitness, so the GAs may get the wrong results. Whereas, when they are too huge, the differences among individuals are weak, so its hard for the selection operator of GAs to select valid individuals with high fitness. Obviously, the traditional GAs are expected to be improved for the constraint optimization problems.

A selection operator of GAs based on direct comparison approach is presented.

Step 1. A function measuring the degree of the individual violating the s.t. is defined. For example,

$$v(x) = -\varepsilon + \sum_{j=1}^{J} g_j(x) \tag{4}$$

where ε is a small positive constant.

Step 2. Choose two individuals, say, $x1$ and $x2$, from previous generation randomly.

Step 3. Select one to the next generation according to the two rules: if $v(x1)$ and $v(x2)$ have the same signs, the one with smaller objective function value is selected; or if $v(x1)$ and $v(x2)$ have different signs, say, $v(x1) < 0$, then $x1$ is selected.

Repeat Step2 and Step3 till the next generation has enough individuals.

This operator treats constraint condition not by penalty functions but by direct comparison, so the advantages of GAs are preserved. Additionally, because it takes the effect of invalid solutions into consideration, the searching ability of GAs is also augmented.

Based on 6DOF nonlinear dynamic model of the robotic airship system, the simulation and optimization program is developed in MATLAB environment. The optimal membership functions of heading error and heading error rate are shown in Fig. 7. Considering the step input of heading error, the airship responses under the optimal fuzzy heading controller and the initial controller are shown in

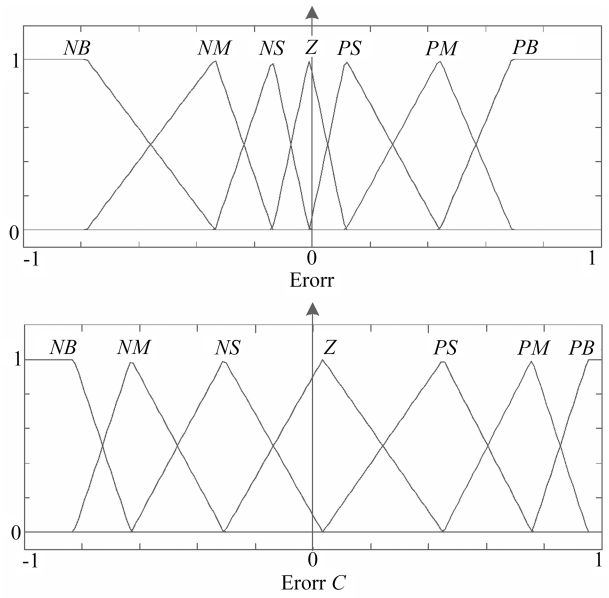

Fig. 7 The optimal membership functions of input variable of heading controller.

Fig. 8. Obviously, the optimal fuzzy heading controller spends much shorter time than the initial one, and overshoot is avoided.

5 Verification of the navigation and control strategies

In the flight experiment, for safety consideration, the elevator and throttle were under manual control to keep the altitude and the cruise speed. The rudder was controlled by the ANN autonomous control system, and it could also be switched to human operator control in take-off and landing phase and in the case of danger.

When the trim airspeed is 8m/s, the tracking error and deflections of rudder are shown in Fig.9. Because of the large time constant and large virtual mass of airship, about 55m tracking errors occurred in two sharp angles despite

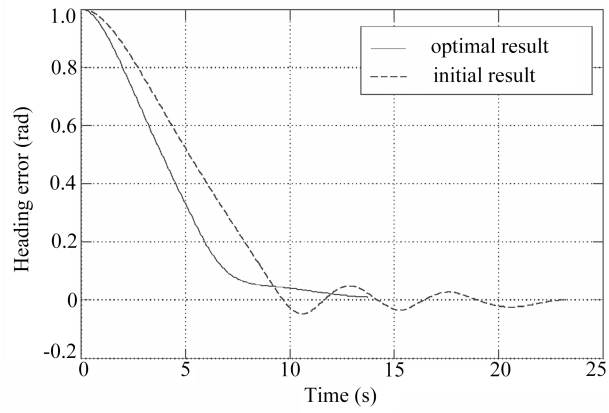

Fig. 8 Responses of the initial fuzzy controller and the optimal fuzzy controller

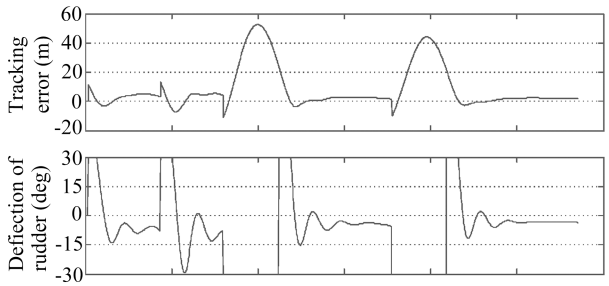

Fig. 9 Tracking error and deflections of rudder

that the saturate control of rudder (+/-30deg) is acted. The results manifest that the strategies are feasible, and the system can track mission path with satisfactory precision.

6 Conclusion

This paper presents computer vision-based navigation and predefined track following control for small robotic airship. The vision system is able to track those visual beacons already existent in the environment. For example, buildings can be used as visual beacons when an airship is flying over a city. According to the digital map or the geographical information system (GIS), their geometrical properties are known. Then a geometrical methodology can extract information about orientation and position of the airship. And in order to keep the airship on a predefined track, a fuzzy flight control system is designed, which uses that data as its inputs. And genetic algorithms (GAs) are utilized to optimize the membership functions of the fuzzy controller.

References

1 Elfes A, Bueno S S, Bergerman M, Paiva E C, Ramos J G, Azinheira J R. Robotic airships for exploration of planetary bodies with an atmosphere: Autonomy challenges. *Autonomous Robots*, 2003, **14**(2∼3): 147∼164

2 Elfes A, Bueno S S, Bergerman M, Ramos J G, Gomes S B V. Project AURORA: Development of an autonomous unmanned remote monitoring robotic airship. *Journal of the Brazilian Computer Society*. 1998, **4**(3): 70∼78

3 Kantora George, Wettergreen David. Collection of environmental data from an airship platform. *Sensor Fusion and Decentralized Control in Robotic Systems*. 2001, **4571**: 76∼83

4 Becker C. Reliable navigation using landmarks. In: Proceedings of the IEEE International Conference on Robotics and Automation. Nagoya, Japan, 1995, **1**: 401∼406

5 Zhang Hong, Ostrowski J. P. Visual servoing with dynamics: Control of an unmanned blimp. In: Proceedings of the IEEE International Conference on Robotics and Automation. Michigan, USA, 1999, **1**: 618∼623

6 Hamel Tarek, Mahony Robert. Visual servoing of an underactuated dynamic rigid-body system: An image-based approach. *IEEE Transactions on Robotics and Automation*, 2002, **18**(2): 187∼198

7 Shakernia Omid, Yi Ma, Koo T J, Hespanha J, Sastry S S. Vision guided landing of an unmanned aerial vehicle. In: Proceeding of the IEEE 38th Conference on Decision and control. Arizon, USA, 1999, **4**: 4143∼4148

8 Azinheira J R, Rives, P, Carvalho J R H, Silvera G F, de Paiva E C, Bueno S S. Visual servo control for the hovering of all outdoor robotic airship. In: Proceedings of the IEEE International Conference on Robotics and Automation. Washington, USA, 2002, **3**: 2787∼2792

9 Rives Patrick, Azinheira J R. Linear structures following by an airship using vanishing point and horizon line in a visual servoing scheme. In: Proceedings of the 2004 IEEE International Conference on Robotics and Automation. New Orleans, USA, 2004, **1**: 255∼260

10 Silveira G F, Garvalho J R H, Rives P, Azinheira J R, Bueno S S, Madrid M K. Optimal visual servoed guidance of outdoor autonomous robotic airships. In: Proceedings of the America Control Conference. USA, 2002, 779∼784
11 Silveira G F, Garvalho J R H, Rives P, Azinheira J R, Bueno S S, Madrid M K. Line following visual servoing for aerial robots combined with complementary sensors. In: Proceedings of the 11th International Conference on Advanced Robotics. Portugal, 2003, 1160∼1165
12 Coelho L S, Campos M F. Pose estimation of autonomous dirigibles using artificial landmarks. In; Proceedings of XII Brazilian Symposium on Computer Graphics and Image Processing. 1999, 161∼170

XIE Shao-Rong Received her Ph. D. degree from Intelligent Machine Institute at Tianjin University in 2001. From 2001 to 2003 she worked as a postdoctoral fellow in Shanghai University. Now she is an associate professor at the same university. Her research interest covers computer vision and intelligent control. Corresponding author of this paper. E-mail: srxie@mail.shu.edu.cn

LUO Jun Associate professor in the school of mechatronics engineering and automation at Shanghai University. He received his Ph. D. degree from the Research Institute of Robotics at Shanghai Jiaotong University in 2000. From 2000 to 2002 he worked as a postdoctoral fellow in Shanghai University. His research interest covers telerobotics and special robotics. E-mail: luojun@shu.eud.cn

RAO Jin-Jun Ph. D. candidate in the School of mechatronics engineering and automation at Shanghai University. His research interest includes flight control of a small robotic airship. E-mail: mrjjrao@yahoo.com.cn

GONG Zhen-Bang Professor at Shanghai University. His research interest covers precision mechanical system and advanced robot. E-mail: zhbgong@shu.edu.cn